Excitations and Stripe Phase Formation in a 2D Dipolar Bose Gas with Tilted Polarization

A. Macia[1], D. Hufnagl[2], F. Mazzanti[1], J. Boronat[1], R. E. Zillich[2]
[1] *Departament de Física i Enginyeria Nuclear, Campus Nord B4-B5, Universitat Politècnica de Catalunya, E-08034 Barcelona, Spain and*
[2] *Institut für Theoretische Physik, Johannes Kepler Universität, Altenbergerstr. 69, 4040 Linz, Austria*

We present calculations of the ground state and excitations of an anisotropic dipolar Bose gas in two dimensions, realized by a non-perpendicular polarization with respect to the system plane. For sufficiently high density an increase of the polarization angle leads to a density instability of the gas phase in the direction where the anisotropic interaction is strongest. Using a dynamic many-body theory, we calculate the dynamic structure function in the gas phase which shows the anisotropic dispersion of the excitations. We find that the energy of roton excitations in the strongly interacting direction decreases with increasing polarization angle and almost vanishes close to the instability. Exact path integral ground state Monte Carlo simulations show that this instability is indeed a quantum phase transition to a stripe phase, characterized by long-range order in the strongly interacting direction.

Strongly correlated dipolar Bose gases in two dimensions (2D) polarized along the direction normal to the system plane have been extensively investigated in recent years [1–4]. The ratio between the dipolar length $r_0 = mC_{dd}/(4\pi\hbar^2)$ and the average interparticle distance provides a measure of the strength of the interaction. C_{dd} is the coupling constant proportional to the square of the (magnetic μ or electric d) dipole moment, resulting in a dipolar length that can range from a few Å for magnetic dipolar systems like ^{52}Cr ($\mu = 6\mu_B$, with μ_B the Bohr magneton), to thousands of Å for heteronuclear polar molecules like KRb, LiCs [5], or RbCs [6]. However, chemical reactions and three-body losses impose limitations on what can be measured in experiments with polar molecules. Therefore, recent efforts focus also on exotic lanthanide magnetic systems like ^{164}Dy or ^{168}Er, [7] where the combined effect of a large magnetic moment ($\mu = 10\mu_B$ for ^{164}Dy and $\mu = 7\mu_B$ for ^{168}Er) and a large mass, lead to dipolar length scales that, although still significantly lower than the corresponding value for polar molecules, is several times larger than that of ^{52}Cr. Er_2 with $\mu = 14\mu_B$ and twice the mass of Er would reach even higher values of r_0 [8].

A 2D dipolar Bose gas polarized along the normal direction to the confining plane develops a roton excitation at high density due to the strong repulsion between dipoles at short distances [3]. Other works have revealed competing effects in a quasi-2D geometry due to the head-to-tail attraction of the dipole-dipole interaction when the third spatial dimension is added, to the point that the system becomes unstable against density fluctuation below a critical trapping frequency in that direction [9–11]. This leads to the question of whether a similar situation can hold in a purely 2D geometry when a head-to-tail component to the dipole-dipole interaction is added by tilting the polarization with respect to the direction normal to the system plane. The interaction becomes anisotropic, $V(\mathbf{r}) = V(x,y) = \frac{C_{dd}}{4\pi r^3}\left[1 - 3\frac{x^2}{r^2}\sin^2\alpha\right]$, with particles moving in the x,y-plane and a polarization field in the x,z-plane, tilted by an angle α with respect to the z-axis. The interaction is weakened in the x-direction as α is increased, while it does not change in the y-direction. Notice that, in the case of bosonic particles, only polarization angles where $V(\mathbf{r})$ is non-negative, i.e. $\alpha \leq \alpha_c = \arcsin(1/\sqrt{3}) = 0.61548\ldots$, are meaningful, if there is no additional short-range repulsion to prevent two dipoles from collapsing to a point.

The effect of a tilted polarization on the superfluid response of a quasi-2D dipolar Bose gas has been investigated by mean field theory [17]. The appearance of a stripe phase has been predicted in 2D dipolar Fermi systems by approximate methods [12–14], observed as a spontaneous symmetry breaking even in the isotropic case ($\alpha = 0$) for high interaction strength. However, recent fixed node diffusion Monte Carlo simulations find no evidence of that in the isotropic case before the system crystallizes [15]. In previous work [16] we investigated the low density regime of the 2D dipolar Bose gas of particles interacting by the potential $V(\mathbf{r})$, analyzing the universal energy scaling properties of the anisotropic gas and other ground state properties. Up to the maximally allowed polarization angle α_c, the low-density system always remains in a gaseous form and no trace of a stripe phase is found. In this work we focus on the high density regimes of this system, studying the effect of the anisotropy on the dispersion relation, especially the roton, and show how a stripe phase forms at large densities and polarization angles. Throughout the paper, lengths and energies are given in units of r_0 and $E_0 = \hbar^2/(mr_0^2)$, respectively.

Before showing exact ground state results obtained by Monte Carlo simulations, we present a qualitative stability analysis of the ground state for a wide range of densities n and polarization angles α. We use the

hyper-netted chain Euler-Lagrange (HNC-EL) [18] technique, which is based on a Jastrow-Feenberg ansatz for the bosonic many-body wave function $\Psi(\mathbf{r}_1,\ldots,\mathbf{r}_N) = \exp\sum_{i<j} u_2(\mathbf{r}_i-\mathbf{r}_j)$. We determine $u_2(\mathbf{r})$ variationally by imposing the extremal condition $\frac{\delta E_g}{\delta\sqrt{g(\mathbf{r})}} = 0$ for the ground state energy E_g and solving for the pair distribution function $g(\mathbf{r})$ within the approximate HNC-EL/0 framework. It was shown in Ref. [19] that when the lowest eigenvalue λ_0 of the hessian $K(\mathbf{r},\mathbf{r}') = \frac{\delta^2 E_g}{\delta\sqrt{g(\mathbf{r})}\delta\sqrt{g(\mathbf{r}')}}$ is non-positive, the system becomes unstable against infinitesimal fluctuations of $g(\mathbf{r})$, where the associated eigenfunction $f_0(\mathbf{r})$ is the fluctuation driving the instability. We have obtained the lowest eigenvalue and eigenvector of $K(\mathbf{r},\mathbf{r}')$ by imaginary-time propagation. Figure 1 shows $\lambda_0(\alpha)$ as function of α for a wide range of densities, where each curve is normalized by the respective isotropic limit, $\lambda_0(0)$. For all n, $\lambda_0(\alpha)$ decreases with increasing α, but there is an important distinction between its behavior at low and high densities: for $n \lesssim 128$, $\lambda_0(\alpha)$ remains finite up to α_c, while for $n \gtrsim 128$ $\lambda_0(\alpha)$ falls to zero already before reaching α_c. Hence the high-density gas state is unstable above a critical angle α_0 which is smaller than α_c; this is also seen by the fact that the HNC-EL equations do not converge in the range $\alpha_0 < \alpha < \alpha_c$. The inset of Fig. 1 shows $f_0(\mathbf{r})$ for $n = 256$ at the largest angle where we found solutions to the HNC-EL equations, $\alpha = 0.58$, where $\lambda_0(\alpha_0)/\lambda_0(0)$ almost vanishes. Away from the correlation hole at $\mathbf{r} = 0$, $f_0(\mathbf{r})$ is essentially a plane wave in the more repulsive y-direction. indicating a tendency of $g(\mathbf{r})$ towards long-range order in the y-direction. We stress that the HNC-EL/0 results become less accurate with larger n, hence the stability limits are only approximate. Exact simulation results are presented below.

The anisotropic nature of the interaction which destabilizes the system beyond α_0 also influences the spectrum of elementary excitations which we investigate by calculating the dynamic structure function $S(\mathbf{k},E)$. $S(\mathbf{k},E)$ is proportional to the probability that a perturbation transfers momentum $\mathbf{k}$ and energy E to the system. Thus, for a given $\mathbf{k}$, $S(\mathbf{k},E)$ has a marked peak if E coincides with the energy of an excitation of the system. We obtain $S(\mathbf{k},E)$ using the dynamic many-body theory [20], where the equations of motion for time-dependent fluctuations of up to pair-correlations in the many-body wave function are solved numerically. If the convolution approximation for the three-body distribution function [21] is used, $S(\mathbf{k},E)$ is obtained as $S(\mathbf{k},E) = -\frac{1}{\pi}\Im m\left[\frac{S(\mathbf{k})}{E-\Sigma(\mathbf{k},E)}\right]$, where $\Sigma(\mathbf{k},E)$ is the complex, energy-dependent self-energy of Eq. (2.46) in Ref. [20]. We note that the only input required to calculate $\Sigma(\mathbf{k},E)$ is the static structure factor $S(\mathbf{k})$ of the ground state.

In order to get exact results for $S(\mathbf{k})$, we have carried out stochastic simulations using the path integral ground state (PIGS) Monte Carlo technique of Ref. [22] which starts from a variational wave function ϕ_0 and projects out components orthogonal to the true ground state by propagation in imaginary time. In this sense, the result of the simulation becomes stochastically *exact* provided the approximation employed for the Green's function is accurate and the propagation time is long enough [23]. In the present case we have used as ϕ_0 a Jastrow-Feenberg ansatz $\prod_{i<j} f(\mathbf{r}_{ij})$ built from the two-body correlation factor $f(\mathbf{r}) = K_0(2/\sqrt{r})$, corresponding to the zero-energy solution of the two-body problem of the isotropic $1/r^3$ interaction. Despite the isotropy of ϕ_0, anisotropic contributions are taken into account by a fourth-order propagator [24], which contains the anisotropic potential $V(\mathbf{r})$ and its gradient. The results presented in this work have been obtained for $N = 512$ particles in a simulation box with periodic boundary conditions. Additionally, simulations with smaller N have been carried out in order to see the N-dependence of the highest peaks in $S(\mathbf{k})$ when n and α increase.

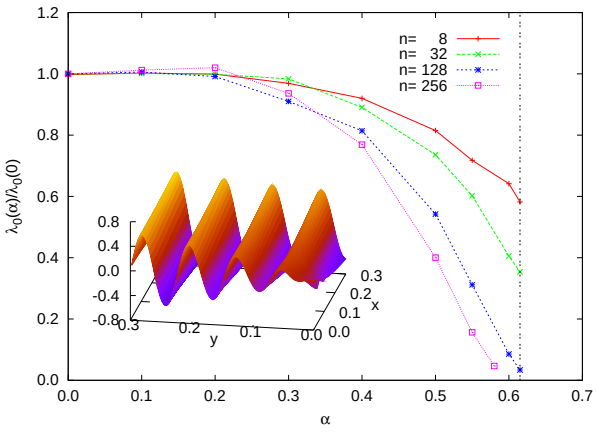

FIG. 1. The lowest eigenvalue $\lambda_0(\alpha)$ of the hessian of the ground state energy E_g is shown in HNC-EL/0 approximation for densities $n = 8; 32; 128; 256$. $\lambda_0(\alpha)$ is normalized by the respective eigenvalue at $\alpha = 0$. The inset shows the eigenfunction $f_0(\mathbf{r})$ for $n = 256$ and $\alpha = 0.58$.

In Ref. 3 we studied the density dependence of $S(\mathbf{k},E)$ of the 2D dipolar quantum gas in the isotropic limit ($\alpha = 0$). There we found a spectrum with a pronounced roton for large density, due to the strong correlations induced by the $1/r^3$ repulsion. Here, we are interested in the dependence of $S(\mathbf{k},E)$ on the polarization angle α and, for a given $\alpha > 0$, its dependence on the direction of $\mathbf{k}$. In Fig. 2, we show $S(\mathbf{k},E)$ for $n = 128$ and $\alpha = 0.20; 0.50; 0.58$ in order to illustrate the evolution from an isotropic to an anisotropic excitation spectrum and the approach to the stability limit. The wave vector $\mathbf{k}$ is pointing in the y and x-direction (i.e. the direction of strongest and weakest interaction) in the left and right panels. We broaden $S(\mathbf{k},E)$ by adding a small imaginary

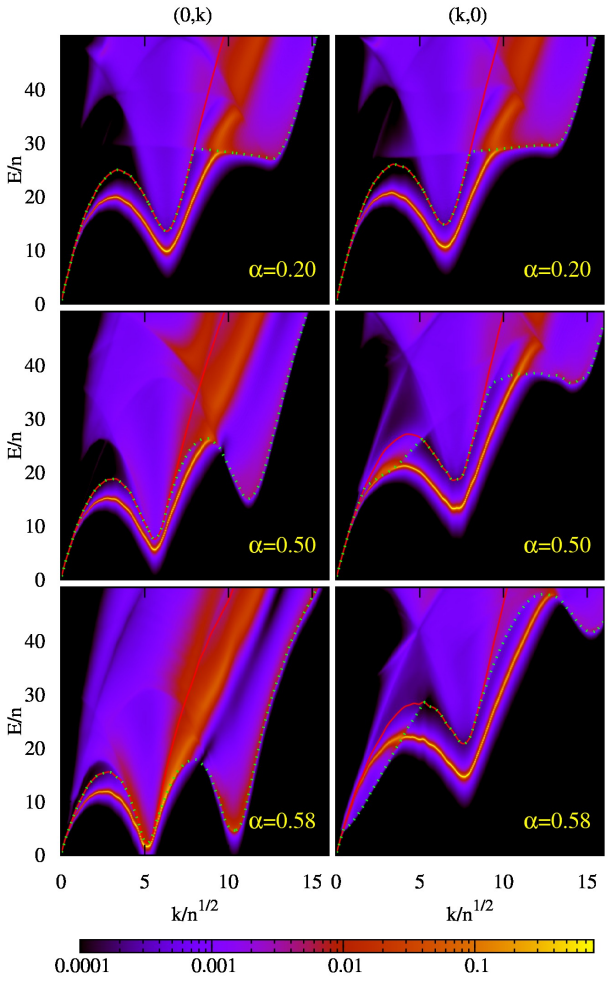

FIG. 2. $S(\mathbf{k}, E)$ for $\mathbf{k} = (0, k)$ (left panels) and $(k, 0)$ (right panels) for polarization angles $\alpha = 0.20; 0.50; 0.58$ at density $n = 128$. The spectrum in Bijl-Feynman approximation is shown as a solid line, and the dotted line denotes the damping limit $E_c(\mathbf{k})$.

part $\eta = 0.2$ to the energy in the calculation of $\Sigma(\mathbf{k}, E)$, since otherwise undamped modes would not be visible in Fig. 2. Also shown is the Bijl-Feynman approximation of the spectrum, obtained by setting $\Sigma(\mathbf{k}, E) = 0$ (solid line).

For $\alpha = 0.20$ the dispersion is almost independent on the direction of $\mathbf{k}$, with only a slight slope of the Pitaevskii plateau [25], which for isotropic systems denotes the sudden onset of damping at twice the roton energy due to decay into two rotons. As α is increased, $S(\mathbf{k}, E)$ becomes very different in the y- and x-direction and features a highly anisotropic dispersion relation for $\alpha = 0.58$. The wave number of the roton depends on the direction of $\mathbf{k}$, but most strikingly its energy decays almost to zero in the y-direction for $\alpha = 0.58$, indicating that the system is close to the limit where the homogeneous gas phase in unstable against infinitesimal density fluctuations. Since the restriction to pair correlation fluctuations used here typically gives an upper bound to the excitation energy [26], the exact roton energy in y-direction is expected to be even smaller. Furthermore, at twice the wave number of the roton, $S(\mathbf{k}, E)$ has another roton-like peak for $\alpha = 0.58$, following a quadratic dispersion, albeit broadened and with smaller spectral weight. In the y-direction, the dispersion relation thus resembles that of a solid, continued beyond the first Brillouin zone. While for $n = 128$ and $\alpha = 0.58$ the system is still in the gas phase, our PIGS results presented below indeed predict a stripe phase at even higher density.

The dotted lines in Fig. 2 depict the damping limit $E_c(\mathbf{k})$ above which decay into two excitations of lower energy is kinematically allowed, hence excitations below $E_c(\mathbf{k})$ have infinite lifetime corresponding to peaks in $S(\mathbf{k}, E)$ with zero linewidth. The kinematics of an anisotropic dispersion is different from the isotropic case, as evidenced e.g. by the lack of a constant Pitaevskii plateau. The decay into two rotons is very efficient in an isotropic system because of the high density of states at the roton energy. For the anisotropic phonon-roton dispersion, the roton energy depends on the direction of $\mathbf{k}$, thus the roton energies are spread out leading to a smoother density of states than in the isotropic limit. For example, decay of the maxon in the y-direction is not allowed, although its energy is higher than twice the roton energy.

Both the results for $S(\mathbf{k}, E)$ and the qualitative stability analysis (Fig. 1) suggest that, as α increases, the system develops a preference for long range order in the y-direction, until the gas phase becomes unstable at a density-dependent critical angle α_0. The PIGS method used to evaluate $S(\mathbf{k})$ in the gas phase can also be used to analyze the static properties of a system with long-range order as the present one when the homogeneous gas is not stable anymore. As in the gas phase, we evaluate $S(\mathbf{k})$ because long-range order can be studied by the emergence of Bragg peaks. This is indeed what happens when α is increased beyond α_0.

Figure 3 summarizes the main PIGS results. The upper left panel shows with black stars the structure factor $S(k)$ (shifted up for better visibility) for the isotropic ($\alpha = 0$) system at $n = 128$, while results along the x- and y-directions for $n = 64$ and $\alpha = 0.58$ are depicted with blue circles and red squares, respectively. $S(k, 0)$ and $S(0, k)$ are markedly different in the anisotropic case, which is a direct consequence of the anisotropy of the interaction induced by the non-vanishing tilting angle. Like in the isotropic case, the system is in the gas phase according to our stability analysis. We visualize this in the upper right panel by a snapshot of one quarter of the simulation box corresponding to the ($n = 64$, $\alpha = 0.58$) case, where each worldline is a different particle. As expected for a gas, there is no apparent ordering.

Results for ($n = 128, \alpha = 0.58$) and ($n = 256, \alpha =$

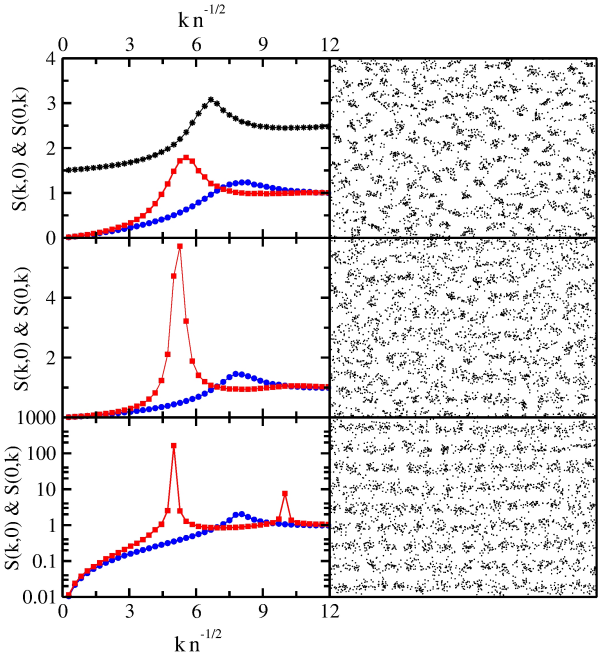

FIG. 3. Static structure factor (left panels) and configuration snapshots (right panels) at different densities and tilting angles. $S(k,0)$ and $S(0,k)$ for $n = 64$ and $\alpha = 0.58$ is shown in the top (blue circles and red squares, respectively). The black stars show the isotropic $S(k)$ at $n = 128$ and $\alpha = 0$. The middle and bottom panels show the $S(k,0$ and $S(0,k)$ and configuration snapshots for $n = 128, \alpha = 0.58$ and $n = 256, \alpha = 0.61$, respectively.

0.61) are shown in the middle and lower panel, respectively. As can be seen, the system becomes more anisotropic for larger density, the peak in $S(0,k)$ is more pronounced, while the peak in $S(k,0)$ is less affected. For $(n = 128, \alpha = 0.58)$ $S(0,k)$ is still a smooth function, with a peak height that is independent of the number of particles N in the simulation. Hence, it is not a Bragg peak and the system is still in the gas phase. However, for $(n = 256$ and $\alpha = 0.61)$, the peak in $S(0,k)$ is orders of magnitude larger than the peak in $S(k,0)$ (notice the logarithmic scale of the bottom panel). The corresponding snapshot shows clearly the formation of a stripe phase, which according to $S(\mathbf{k})$ is like a gas in the x-direction where the interaction is weak, and a solid along the y-axis where the interaction is strong. The peak in $S(0,k)$ grows almost linearly with N, which further supports its interpretation as a Bragg peak. A second peak of less but still significant intensity develops at twice the wave number of the first peak. We note that for $\alpha = 0$ a stripe phase has not been observed and the isotropic system remains in the gas phase until it solidifies at high density [2]. The same conclusion for a fully isotropic interaction has been reported recently for a dipolar Fermi gas in 2D [15].

We close the discussion showing a 3D-map of the pair distribution function $g(\mathbf{r})$ for $|\mathbf{r}| < L_-/2$ (L_- is the

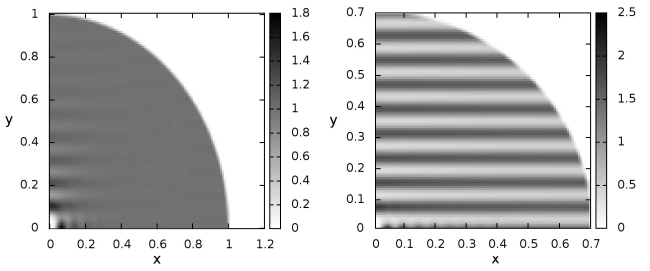

FIG. 4. Pair distribution function $g(x,y)$ for density $n = 128$ and $\alpha = 0.58$ (left), and for $n = 256$ and $\alpha = 0.61$ (right).

smaller side of the simulation box) in Fig. 4 for the two cases $(n = 128, \alpha = 0.58)$ (left panel) and $(n = 256, \alpha = 0.61)$ (right panel). The stripe phase becomes clearly visible in the second case as a plane wave in the y-direction, filling the whole simulation box. For $(n = 128, \alpha = 0.58)$ oscillations in the y-direction are present only for small x and are damped with increasing y, hence $g(\mathbf{r})$ becomes isotropic for large $|\mathbf{r}|$ and equal to unity, consistent with the behavior of a gas.

Summarizing, we have analyzed the behavior of an anisotropic dipolar Bose gas in 2D, using several methods: a qualitative stability analysis of the ground state based on the HNC-EL method, the exact calculation of structural quantities from PIGS Monte Carlo simulations, and the dynamic structure function in the pair fluctuation approximation of the dynamic many-body theory. All results show that for large tilting angle α and large density n, there is a quantum phase transition to a stripe phase, characterized by long-range order in the direction of stronger interaction. The phonon-roton dispersion is very anisotropic in the gas phase close to the stripe phase transition, with an almost vanishing roton energy in the y-direction.

This work has been supported by the Austrian Science Foundation FWF under grant No. 23535, and by Grant No. FIS2011-25275 from DGI (Spain) and Grant No. 2009-SGR1003 from the Generalitat de Catalunya (Spain). D.H. and R.E.Z are grateful to E. Krotscheck for helpful discussions

[1] K. I. Golden, G. J. Kalman, P. Hartmann, and Z. Donkó, Phys. Rev. E **82**, 036402 (2010).
[2] G. E. Astrakharchik, J. Boronat, I. L. Kurbakov, and Y. E. Lozovik, Phys. Rev. Lett. **98**, 060405 (2007).
[3] F. Mazzanti, R. E. Zillich, G. E. Astrakharchik, and J. Boronat, Phys. Rev. Lett. **102**, 110405 (2009).
[4] A. Filinov, N. V. Prokofev, and M. Bonitz, Phys. Rev. Lett. **105**, 070401 (2010).
[5] K. K. Ni, S. Ospelkaus, D. J. Nesbitt, J. Ye, and D. S. Jin, Phys. Chem. Chem. Phys. **11**, 9626 (2009).

[6] T. Takekoshi, M. Debatin, R. Rameshan, F. Ferlaino, R. Grimm, H.-C. Nägerl, C. R. Le Sueur, J. M. Hutson, P. S. Julienne, S. Kotochigova, and E. Tiemann, Phys. Rev. A **85**, 032506 (2012).

[7] K. Aikawa, A. Frisch, M. Mark, S. Baier, A. Rietzler, R. Grimm, and F. Ferlaino, Phys. Rev. Lett. **108**, 210401 (2012).

[8] F. Ferlaino, private communication.

[9] L. Santos, G. Shlyapnikov, and M. Lewenstein, Phys. Rev. Lett. **90**, 250403 (2003).

[10] R. M. Wilson, S. Ronen, J. L. Bohn, and H. Pu, Phys. Rev. Lett. **100**, 245302 (2008).

[11] D. Hufnagl, R. Kaltseis, V. Apaja, and R. E. Zillich, Phys. Rev. Lett. **107**, 065303 (2011).

[12] Y. Yamaguchi, T. Sogo, T. Ito, and T. Miyakawa, Phys. Rev. A **82**, 013643 (2010).

[13] M. M. Parish and F. M. Marchetti, Phys. Rev. Lett. **108**, 145304 (2012).

[14] K. Sun, C. Wu, and S. Das Sarma, Phys. Rev. B **82**, 075105 (2010).

[15] N. Matveeva and S. Giorgini, arXiv:1206.3904v1 (2012).

[16] A. Macia, F. Mazzanti, J. Boronat, and R. E. Zillich, Phys. Rev. A **84**, 033625 (2011).

[17] C. Ticknor, R. M. Wilson, and J. L. Bohn, Phys. Rev. Lett. **106**, 065301 (2011).

[18] A. Polls and F. Mazzanti, in *Introduction to Modern Methods of Quantum Many-Body Theory and Their Applications*, Series on Advances in Quantum Many Body Theory Vol.7, edited by A. Fabrocini, S. Fantoni, and E. Krotscheck (World Scientific, 2002) p. 49.

[19] L. Castillejo, A. D. Jackson, B. Jennings, and R. A. Smith, Phys. Rev. B **20**, 3631 (1979).

[20] C. E. Campbell and E. Krotscheck, Phys. Rev. B **80**, 174501 (2009).

[21] E. Feenberg, *Theory of Quantum Fluids* (Academic Press, 1969).

[22] A. Sarsa, K. E. Schmidt, and W. R. Magro, J. Chem. Phys. **113**, 1366 (2000).

[23] R. Rota, J. Casulleras, F. Mazzanti, and J. Boronat, Phys. Rev. E **81**, 016707 (2010).

[24] J. E. Cuervo, P. N. Roy, and M. Boninsegni, J. Chem. Phys. **122**, 114504 (2005).

[25] L. P. Pitaevskii, Zh. Eksp. Teor. Fiz. **36**, 1169 (1958).

[26] C. E. Campbell and E. Krotscheck, J. of Low Temp. Phys. **158**, 226 (2010).